International Journal of Economy, Energy and Environment
2026, Vol. 11, No. 3, pp. 46–58
https://doi.org/10.11648/j.ijeee.20261103.11

Research Article

Sodium Dodecyl Sulfate and Calcium Hydroxide Exhibit a Synergistic Effect in Promoting the Formation of Carbon Dioxide Hydrate

Yaxiong Yang[1], Yuxin Jia[1], Xiaolong Zhu[1], Lei Yang[1, 2, *], Yongchen Song[1]

[1]Key Laboratory of Ocean Energy Utilization and Energy Conservation of Ministry of Education, Dalian University of Technology, Dalian, China

[2]Ningbo Institute of Dalian University of Technology, Dalian University of Technology, Ningbo, China

Abstract

The continuous increase in carbon dioxide (CO_2) emissions has raised serious environmental concerns, highlighting the urgent need for efficient carbon capture, utilization, and storage (CCUS) technologies. Among the available approaches, CO_2 hydrate-based sequestration has attracted significant attention due to its high gas storage capacity, mild operating conditions, and environmental compatibility. However, its practical application remains hindered by slow formation kinetics, long induction times, and low gas consumption efficiency. In this study, a novel synergistic promotion strategy was proposed to simultaneously enhance both the formation kinetics and gas storage performance of CO_2 hydrates. Calcium hydroxide ($Ca(OH)_2$) was introduced as a reactive additive, which reacts with CO_2 to generate calcium carbonate ($CaCO_3$) particles in situ. These $CaCO_3$ particles effectively shorten the hydrate induction period by providing favorable nucleation sites. Meanwhile, sodium dodecyl sulfate (SDS), a typical surfactant, was employed to modify the surface properties of $CaCO_3$ particles. The adsorption of SDS onto the $CaCO_3$ surface enhances its hydrophobicity, thereby improving gas–liquid contact and promoting hydrate nucleation and growth. The experimental results demonstrate that the addition of $Ca(OH)_2$ or SDS alone significantly reduces the induction time by up to 91.4% and 82.98%, respectively, compared with pure water. However, their effects on hydrate formation rate and gas consumption are limited. In contrast, the combined SDS–$Ca(OH)_2$ system exhibits a pronounced synergistic effect. The induction time is reduced by 88.16%, while the hydrate formation rate and gas consumption are significantly enhanced by 739.13% and 276.19%, respectively. This study provides an effective and promising strategy for improving CO_2 hydrate formation performance, offering strong potential for large-scale applications in carbon capture and storage.

Keywords

Carbon Dioxide Hydrate, Kinetic Promoter, Carbon Sequestration

*Correspondence: Lei Yang (leiyang@dlut.edu.cn)

Received: 13 April 2026; **Accepted:** 20 April 2026; **Published:** 8 May 2026

1. Introduction

Greenhouse gas emissions have caused global warming, posing severe threats to the human living environment. Carbon dioxide (CO_2), primarily produced from fossil fuel combustion and industrial processes, is a major contributor to these emissions. However, given the continued reliance on fossil fuels in today's industrialized world, completely eliminating CO_2 emissions is impractical. Therefore, developing efficient and stable methods for CO_2 capture and storage has become a critical scientific and engineering challenge in the global energy and environmental sectors.

CO_2 hydrates represent a promising technology for carbon capture and storage. As a type of gas hydrate, CO_2 hydrate forms under low-temperature and high-pressure conditions, where water molecules are linked via hydrogen bonds to create a cage-like lattice structure. Within this structure, CO_2 molecules are physically encapsulated in the lattice cavities without forming chemical bonds, exhibiting the characteristic host–guest arrangement: water molecules constitute a stable lattice framework (host), while CO_2 molecules occupy the cavity sites (guest) [1]. Under ideal conditions, when the hydrate cavities are fully occupied by CO_2 molecules, 1 cubic meter of CO_2 hydrate can sequester 164 cubic meters of CO_2 gas at standard conditions, highlighting the significant potential of hydrate-based CO_2 storage.

Although CO_2 hydrates hold great potential for carbon capture and storage, their practical application is hindered by slow formation rates and limited hydrate yield. Therefore, investigating methods to enhance the formation kinetics of CO_2 hydrates is crucial for their practical utilization. Many researchers have developed various types of kinetic promoters aimed at increasing both the formation rate and the yield of CO_2 hydrates.

The effects of surfactants on gas hydrate growth have been extensively studied [2-6], including anionic, nonionic, and cationic surfactants. Kumar et al. investigated the influence of three surfactants (Tween-80, Dodecyltrimethylammonium Chloride (DTACI), and SDS) on CO_2 gas hydrates and found that anionic (SDS) and nonionic (Tween-80) surfactants significantly outperformed the cationic surfactant (DTACI) in promoting CO_2 hydrate formation, with SDS showing the best performance [7]. Molokitina et al. studied the formation of CO_2 hydrates in the presence of SDS and found that the effect of SDS on the CO_2 growth mechanism depends on the mass transfer driving force and does not affect CO_2 solubility in water. Their experiments showed that high CO_2 hydrate conversion ratio were only achieved under low mass transfer driving forces and quiescent conditions, whereas at high driving forces, SDS had no significant effect on hydrate growth [8]. Partoon et al. experimentally studied SDS as a promoter for CO_2 hydrate formation and demonstrated that the presence of SDS shortened the induction time and facilitated hydrate nucleation [9]. Ganji et al. investigated the effects of the anionic surfactants SDS and linear alkylbenzene sulfonate (LABS), the cationic surfactant cetyltrimethylammonium bromide (CTAB), and the nonionic surfactant ethoxylated nonylphenol (ENP) on methane hydrate formation, dissociation, and storage capacity. The results indicated that SDS had the most pronounced effect on the methane hydrate formation rate while also enhancing storage capacity [10]. These studies indicate that surfactants significantly influence hydrate formation, with SDS being particularly effective in reducing the induction time of CO_2 hydrates and also showing excellent promotion of methane hydrate formation.

Nanoparticles, including metal nanoparticles, metal oxide nanoparticles, and carbon-based nanomaterials, have also been widely applied in gas hydrate formation [11-16]. Mohammadi et al. investigated the effect of a mixture of SDS and silver nanoparticles on CO_2 hydrate formation, and the results showed that the mixture had no significant effect on the hydrate induction time but effectively increased CO_2 consumption and the consumption rate [17]. Zhou et al. found that graphite nanoparticles could significantly shorten the induction time of CO2 hydrates and increase the maximum CO_2 consumption [18]. Liu et al. studied the effect of a mixed additive composed of sodium dodecyl sulfate (SDS), tetrahydrofuran (THF), and graphene oxide (GO) on CO_2 hydrate formation. The experiments indicated that using GO alone did not significantly enhance CO_2 consumption, whereas the mixed additive shortened the hydrate formation time and substantially increased gas consumption [19].

Nanoparticles can significantly improve the heat transfer properties of the fluid, facilitating the release of heat during hydrate formation, which in turn promotes the formation kinetics of hydrates.

Studies have shown that the surface properties of particles also affect gas hydrate formation [20-23]. Farhang et al. found that hydrophobic fumed silica particles could enhance the formation kinetics of CO_2 hydrates [24]. Deng et al. investigated the effect of hydrophobic fluorinated graphite and its combination with SDS on CO_2 hydrate formation. The results indicated that the superhydrophobicity and nanostructure of fluorinated graphite effectively promoted hydrate formation, and the best promotion effect was achieved when combined with 300 ppm SDS [25]. Nguyen et al. studied the relationship between surface hydrophobicity, solid–water interfacial properties, and hydrate formation through molecular dynamics simulations and experiments. Their findings showed that hydrophobic surfaces increase local gas density and induce local ordering of water molecules near the hydrophobic solid surface, leading to preferential hydrate formation on hydrophobic surfaces [22].

Besides CO_2 hydrate technology, mineralization is another promising approach for CO_2 sequestration. Gao et al. employed amino acids to enhance the leaching of calcium ions from industrial waste (calcium carbide slag), with L-serine achieving the highest leaching rate of 90.6%. thereby promoting the mineralization process [26]. The main component of calcium carbide slag is calcium oxide, and the leachate primarily contains

$Ca(OH)_2$, which reacts with CO_2 to achieve carbon fixation. The calcium carbonate produced from the reaction between $Ca(OH)_2$ and CO_2 can also facilitate the nucleation of CO_2 hydrates. Cheng et al. utilized $Ca(OH)_2$ in combination with tetrafluoroethane to promote CO_2 hydrate formation. Their experiments showed that the $CaCO_3$ particles generated from the reaction of $Ca(OH)_2$ with CO_2 significantly induce and accelerate hydrate formation, and in the presence of tetrafluoroethane, CO_2 consumption increased by 50% [27]. Therefore, adding $Ca(OH)_{2-}$ not only consumes CO_{2-} through reaction with CO_{2-}, but the generated $CaCO_3$ particles also promote the formation of CO_{2-} hydrates.

Although these studies have effectively enhanced the formation rate and yield of CO_2 hydrates, there is still room for improvement in achieving efficient CO_2 sequestration. In this study, we aim to promote CO_2 hydrate formation synergistically by combining particles generated from CO_2 mineralization with the surfactant sodium dodecyl sulfate (SDS).

2. Experimental Section

2.1. Experimental Materials

High-purity carbon dioxide (99.99%) used in this study was supplied by Dalian Specialty Gas Co., Ltd. (Dalian, China). Sodium dodecyl sulfate (SDS, molecular formula $NaC_{12}H_{25}SO_4$, 99% purity) and calcium hydroxide ($Ca(OH)_2$, 95% purity) were purchased from Shanghai Macklin Biochemical Technology Co., Ltd. (Shanghai, China). Deionized water (DIW) used in the experiments was prepared using a laboratory ultrapure water system (Aquapro2S, Aquapro International Company LLC, USA), which produces DIW with a resistivity of 18.2 MΩ·cm.

2.2. Experimental Equipment

The experimental setup used in this study is shown in Figure 1. Hydrate formation occurred in a stainless-steel reactor with an effective volume of 117.81 cm³, capable of withstanding pressures up to 20 MPa. The reactor was equipped with a temperature sensor (PT100), a pressure sensor, and valves for gas charging and venting. The measurement accuracies of the temperature and pressure sensors were ± 0.01 ℃ and ± 0.01 MPa, respectively. During the experiment, the reactor temperature and pressure were recorded every 30 seconds by a data acquisition system and transmitted to a desktop computer. The reactor was immersed in a circulating water bath (Polyscience, USA) for temperature control.

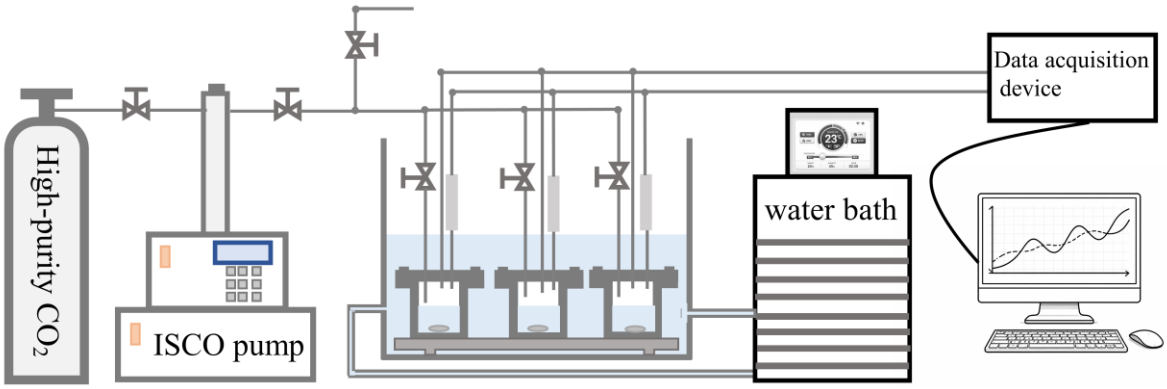

Figure 1. *Schematic diagram of the CO_2 hydrate formation test bench.*

2.3. Experimental Steps

Before each experiment, the reactor was thoroughly cleaned with deionized water and evacuated using a vacuum pump to remove air. A magnetic stirrer was placed inside the reactor, and the stirring speed was set to 600 r/min. The required solution was first prepared and injected into the reactor. The reactor was then placed in the circulating water bath until it reached the set temperature. CO_2 gas was subsequently injected into the reactor until the pressure reached 3.6 MPa. After waiting for one hour to allow complete CO_2 dissolution and reaction, additional CO_2 gas was supplied to maintain the reactor pressure at 3.6 MPa. The water bath temperature was then set to 275.15 K to initiate cooling. The experiment continued for 1000 min, after which it was terminated. Each experiment was repeated three times.

3. Calculation Method

Since hydrate formation is an exothermic process, the onset of hydrate formation can be identified by a rise in the temperature recorded by the sensor. In this study, the induction time is defined as the time interval from the start of cooling to the point at which a sudden increase in the temperature sensor reading is observed. The induction time is expressed in minutes. If no temperature rise is detected during an experiment, the induction time is considered to be 1000 min. Each

experiment was repeated three times, and the average value was reported.

The gas consumption (Δn_{gas}) during CO_2 hydrate formation was calculated using Equations (1-3).

$$\Delta n_{gas} = n_{0,gas} - n_{t,gas} \quad (1)$$

$$n_{0,gas} = \frac{P_{0,gas}V_{0,gas}}{Z_0RT_0} \quad (2)$$

$$n_{t,gas} = \frac{P_{t,gas}V_{t,gas}}{Z_tRT_t} \quad (3)$$

Here, $n_{0,gas}$ represents the amount of CO_2 gas in the reactor at the initial time, and $n_{t,gas}$represents the amount of CO_2 gas at time t. $P_{0,gas}$and $P_{t,gas}$ denote the CO_2 gas pressures in the reactor, which can be directly measured by the pressure sensor. $V_{0,gas}$ and $V_{t,gas}$ represents the CO_2 gas volume in the reactor, and can be calculated using Equations (4) and (5).

$$V_{0,gas} = V_{whole} - V_{0,water} - V_{Ca(OH)_2} \quad (4)$$

$$V_{t,gas} = V_{0,gas} - (V_{t,hydrate} - V_{t,water}) \quad (5)$$

V_{whole} represents the total effective internal volume of the reactor, which is 117.81 cm^3. $V_{0,water}$ denotes the volume of the solution added. In the calculations, the density of water is taken as 0.997 $g \cdot cm^{-3}$. The effect of SDS addition on the density of water is neglected, and the densities of water are used directly in the calculations.

$V_{Ca(OH)_2}$ represents the volume of $Ca(OH)_2$ added. Due to its limited solubility, $Ca(OH)_2$ occupies a portion of the reactor volume when added to the solution. In the laboratory, measurements using a graduated cylinder show that the volume of 1 g of $Ca(OH)_2$ powder (uncompacted) is approximately 1.5 cm^3, and the volume for different masses of $Ca(OH)_2$ is calculated proportionally based on its mass.

Z represents the compressibility factor, and Z_0 and Z_t can be calculated using Equation (6). R denotes the universal gas constant, taken as 8.314 $J \cdot mol^{-1} \cdot K^{-1}$. T_0 and T_t represent the temperatures at the initial time and at time t, respectively, which can be directly measured by the temperature sensor.

$$Z = 1 + \left[0.083 - 0.422 \times \left(\frac{T_c}{T}\right)^{1.6}\right]\frac{PT_c}{P_cT} + \omega\left[0.139 - 0.172 \times \left(\frac{T_c}{T}\right)^{4.2}\right]\frac{PT_c}{P_cT} \quad (6)$$

Here, T_c is the critical temperature, which is 304.2 K for CO_2; P_c is the critical pressure, with a value of 7.376 MPa for CO_2; and ω is the acentric factor, which is 0.225. P and T represent the gas pressure and temperature, respectively.

$V_{t,hydrate}$ represents the hydrate volume at time t, and $V_{t,water}$ denotes the volume of water consumed for hydrate formation at time t. $V_{t,hydrate}$ can be calculated using Equation (7).

$$V_{t,hydrate} = \frac{\alpha(n_{0,gas} - n_{t,gas})xM_{water}}{\rho_{water}} \quad (7)$$

α represents the volume expansion factor of water upon hydrate formation, which is taken as 1.25 in this study [28].x denotes the hydration number, with a value of 6.04 adopted in this work, as determined by Kumar et al. using infrared spectroscopy and gas chromatography [29]. M_{water} is the molar mass of water, with a value of 18 $g \cdot mol^{-1}$.

$n_{t,gas}$ can be calculated using Equations (2-5) and (7).

$$n_{t,gas} = \frac{P_{t,gas}(V_{0,gas} - n_{0,gas}(\alpha-1)xM_{water}/\rho_{water})}{Z_{t,gas}RT_{t,gas} - P_{t,gas}(\alpha-1)xM_{water}/\rho_{water}} \quad (8)$$

The gas consumption rate ($r_{t,gas}$) in the experiment is defined as the amount of CO_2 consumed every 5 minutes, with a unit of $mol \cdot min^{-1}$, and is calculated according to Equation (9).

$$r_{t,gas} = \frac{n_{t,gas} - n_{t+5,gas}}{5} \quad (9)$$

The gas reaction ratio (R_{gas}) is defined as the ratio of gas consumption to the initial gas amount. A higher value indicates a greater proportion of gas consumption. The calculation method is as follows:

$$R_{gas} = \frac{\Delta n_{gas}}{n_{0,gas}} \quad (10)$$

The water conversion ratio (W_c) is defined as the percentage of water converted into hydrates, which reflects the extent of water consumption during the experiment.

$$W_c = \frac{x\Delta n_{gas}}{n_{water}} \quad (11)$$

The gas uptake capacity (s) is defined as the volume of CO_2 consumed at standard conditions per unit volume of water, which directly reflects the CO_2 storage capacity.

$$s = \frac{2240 \times \Delta n_{gas}}{V_{water}} \quad (12)$$

4. Results and Discussion

4.1. Effect of Single Additives on CO_2 Hydrate Formation

To investigate the individual effects of $Ca(OH)_2$ and SDS on CO_2 hydrate formation, different amounts of $Ca(OH)_2$ or SDS were added to 50 g of deionized water. The specific experimental conditions are listed in Table 1.

Table 1. *Experimental conditions for single-additive systems.*

Experiment	H_2O Mass (g)	SDS Mass (g)	$Ca(OH)_2$ Mass (g)	Temperature (°C)	Pressure (MPa)
Case 1	50	0	0	2	3.6
Case 2	50	0	0.05	2	3.6
Case 3	50	0	0.1	2	3.6
Case 4	50	0	0.5	2	3.6
Case 5	50	0	1	2	3.6
Case 6	50	0.005	0	2	3.6
Case 7	50	0.01	0	2	3.6
Case 8	50	0.05	0	2	3.6
Case 9	50	0.1	0	2	3.6
Case 10	50	0.3	0	2	3.6

Since hydrate formation is an exothermic process, the onset of hydrate formation is indicated by a sudden rise in the temperature sensor reading. In this study, the induction time of hydrate formation is defined as the time elapsed from the start of cooling of the circulating water bath to the first observed temperature jump. Due to the stochastic nature of hydrate formation, the measured induction time exhibits some variability. If no temperature increase is observed during an experiment, the induction time is assigned a value of 1000 minutes, and the average of three repeated experiments is used.

The induction times were measured for pure water, various SDS concentrations, and different amounts of $Ca(OH)_2$. As shown in Figure 2, the induction time of CO_2 hydrate in pure water is approximately 752 minutes. The addition of SDS at different concentrations significantly reduced the induction time, exhibiting a trend of "initial shortening followed by extension" with increasing SDS concentration, consistent with the findings of Partoon et al. [9]. At an SDS concentration of 1000 ppm, the induction time is minimized, with relatively low fluctuation. At very low or very high SDS concentrations, the reduction in induction time is less pronounced, likely due to the effects of SDS on the gas–liquid interface.

Since CO_2 hydrates form at the gas–liquid interface, low SDS concentrations may hinder the aggregation of hydrate particles at the interface, suppressing further growth. With increasing SDS concentration, gas–liquid interactions are enhanced, the number of hydrate nuclei increases, and the induction time shortens. When the SDS concentration exceeds the critical micelle concentration, excess SDS predominantly exists as micelles, the effective monomer concentration at the interface saturates, and the gas–liquid interface is covered by a dense adsorption layer. This increases interfacial mass transfer resistance, limits nucleation, and consequently extends the induction time.

The addition of different mass fractions of $Ca(OH)_2$ significantly reduced the induction time of hydrate formation compared to pure water. Nesterov et al. reported that promoter particles containing carbon-based groups, including carbonates, can markedly shorten the induction time of gas hydrates, and the induction time decreases with increasing particle size [30]. In this study, the added $Ca(OH)_2$ reacted with CO_2 to form $CaCO_3$, and the presence of carbonates effectively shortened the induction time. Furthermore, Cheng et al. found that $CaCO_3$ particles generated from the reaction of $Ca(OH)_2$ with CO_2 provide additional nucleation sites, further reducing the induction time [27]. When 0.5 g of $Ca(OH)_2$ was added, the induction time decreased to 64.67 minutes. However, further increasing the $Ca(OH)_2$ amount led to a longer induction time, likely due to the formation of a $CaCO_3$ film at the gas–liquid interface, which reduces the area available for hydrate particle formation and thereby hinders hydrate growth.

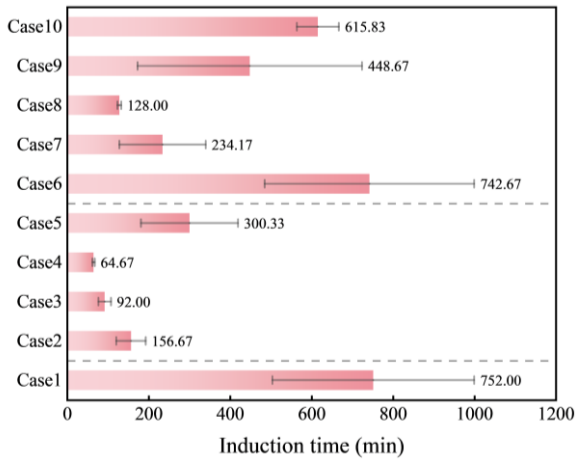

Figure 2. *Induction time of CO_2 hydrate formation in a single system.*

Figure 3 illustrates the changes in the amount of CO_2 in the reactor during the experiment. The remaining CO_2 indicates that most of the CO_2 consumption occurs during the cooling stage, where the decrease in temperature increases CO_2 solubility, leading to a reduction in gas phase CO_2. In single-additive systems, the amount of CO_2 consumed due to hydrate formation is relatively small in most experiments, and the gas consumption process is slow. Under pure water conditions, the CO_2 consumption is approximately 22 mM.

For SDS added systems, the CO_2 consumption at the lowest and highest SDS concentrations is slightly lower than that in pure water, consistent with the observed increase in induction time at these concentrations. At other SDS concentrations, the CO_2 consumption slightly increases; however, overall, single SDS addition has no significant effect on CO_2 hydrate production. This observation aligns with the findings of Molokitina et al.: when the supercooling exceeds 2°C, SDS has no noticeable effect on hydrate growth even under laminar stirring [8]. This may be attributed to the high solubility of CO_2 in water, as hydrate growth primarily occurs at the liquid side of the hydrate film from dissolved CO_2. The formation of a dense hydrate film inhibits further growth that relies on capillary-driven mechanisms.

When different amounts of $Ca(OH)_2$ are added, most of the CO_2 consumption still occurs during the cooling stage. Only at the addition of 0.05 g $Ca(OH)_2$ does hydrate formation get promoted, resulting in increased gas consumption. Han et al. investigated the effects of saturated and supersaturated $Ca(OH)_2$ solutions on CO_2 absorption, finding that undissolved $Ca(OH)_2$ in the suspension hinders CO_2 dissolution [31]. Therefore, in this study, low concentrations of $Ca(OH)_2$ (unsaturated solution) can enhance CO_2 solubility, thereby promoting hydrate formation. However, at higher mass fractions, $Ca(OH)_2$ suspensions impede CO_2 dissolution, reducing the availability of guest molecules during hydrate formation, which decreases the amount of CO_2 hydrate formed and lowers CO_2 consumption. In addition, $CaCO_3$ particles generated from low-mass-fraction $Ca(OH)_2$ can provide additional nucleation sites, promoting hydrate formation. Yet, when $Ca(OH)_2$ exists as a suspension, the resulting $CaCO_3$ particles carry a weak positive surface charge [32], causing water molecules to accumulate near the particles and obstructing the formation of hydrate cage structures, thereby inhibiting hydrate growth.

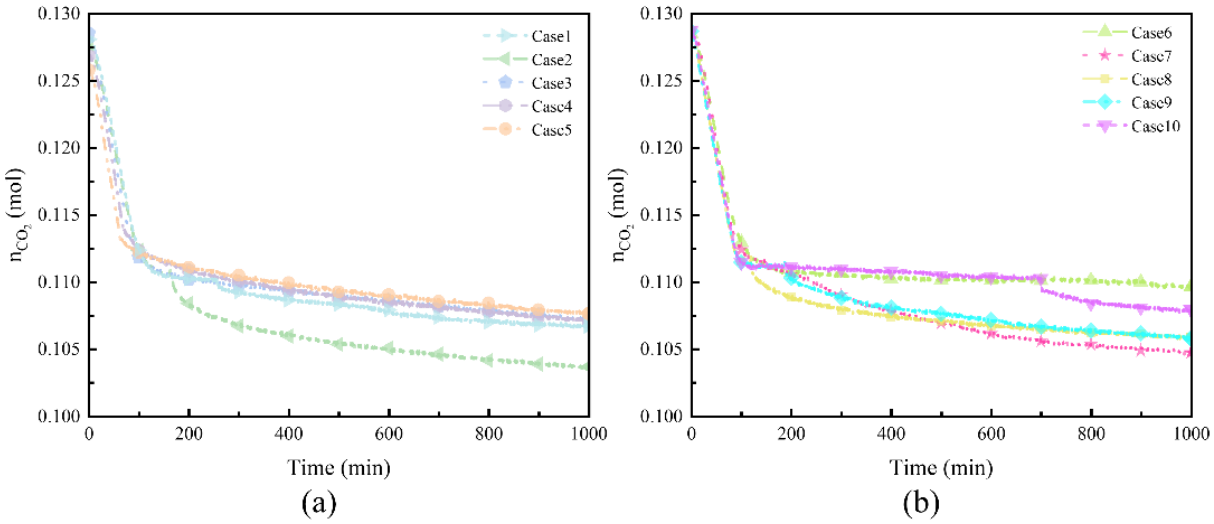

Figure 3. *CO_2 gas amount in the reactor under varying $Ca(OH)_2$ and SDS dosages: (a) $Ca(OH)_2$ dosage; (b) SDS dosage.*

Figure 4 presents the CO_2 gas consumption rate and total gas consumption under conditions with different amounts of $Ca(OH)_2$ and various concentrations of SDS as single additives. The gas consumption rate curve has been smoothed, therefore the maximum gas consumption rate cannot be reflected in the graph. Table 2 shows the maximum rate of carbon dioxide consumption and the final amount consumed. Since gas consumption in both pure water and single-additive systems mainly occurs during the cooling stage, and the cooling rate of the circulating water bath remains the same, the maximum gas consumption rates are similar across all systems, approximately 0.23 mmol·min^{-1}. Under pure water conditions, the maximum gas consumption rate during the hydrate formation stage is 0.102 mmol·min^{-1}. When 0.05 g of $Ca(OH)_2$ is added, the maximum rate increases to 0.163 mmol·min^{-1}, whereas it is only 0.08 mmol·min^{-1} when 0.1 g of SDS is added. These results indicate that SDS alone does not significantly enhance the formation rate of CO_2 hydrates, while $Ca(OH)_2$ shows a limited promotion effect. From the gas consumption curves, it can be observed that, apart from the cooling stage, the total gas consumption remains low and the process is relatively slow in pure water as well as in systems with only SDS or $Ca(OH)_2$. This suggests that large-scale and rapid formation of CO_2 hydrates cannot be achieved under these conditions.

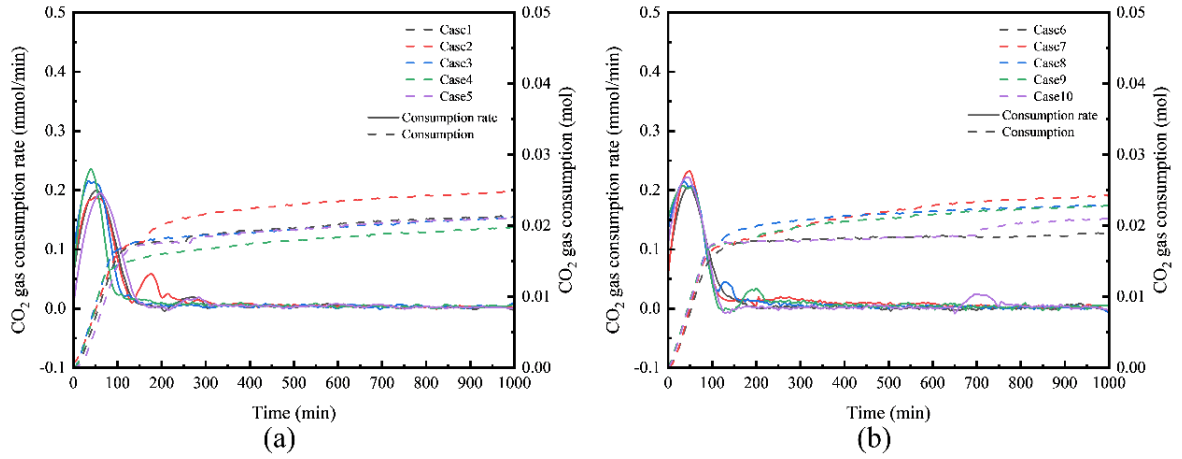

Figure 4. *CO_2 consumption and consumption rate with single addition of SDS or $Ca(OH)_2$: (a) different masses of $Ca(OH)_2$; (b) different masses of SDS.*

Table 2. *Maximum rate of carbon dioxide consumption and final consumption.*

Experiment	Maximum carbon dioxide consumption (mmol·min^{-1})	carbon dioxide final consumption (mol)
Case 1	0.231	0.022
Case 2	0.211	0.025
Case 3	0.227	0.021
Case 4	0.26	0.02
Case 5	0.197	0.021
Case 6	0.223	0.019
Case 7	0.242	0.024
Case 8	0.237	0.023
Case9	0.238	0.023
Case 10	0.235	0.021

Figure 5 illustrates the water conversion ratio, gas reaction ratio, and gas uptake capacity of CO_2 hydrates under different single-additive conditions. It can be observed that, with increasing $Ca(OH)_2$ dosage, the water conversion ratio, gas reaction ratio, and gas uptake capacity generally show a decreasing trend, and a clear inhibitory effect appears at higher dosages. When SDS is added at different concentrations, the gas uptake capacity shows a slight increase; however, the overall promotion effect is not significant. In addition, at an SDS concentration of 200 ppm, relatively large fluctuations are observed in repeated experiments, although both water conversion ratio and gas reaction ratio reach relatively high values under this condition. In the system with $Ca(OH)_2$ as the sole additive, the gas uptake capacity shows a slight increase when 0.05 g of $Ca(OH)_2$ is added. This enhancement is mainly attributed to the increased solubility of CO_2 under this condition, which primarily occurs during the cooling stage.

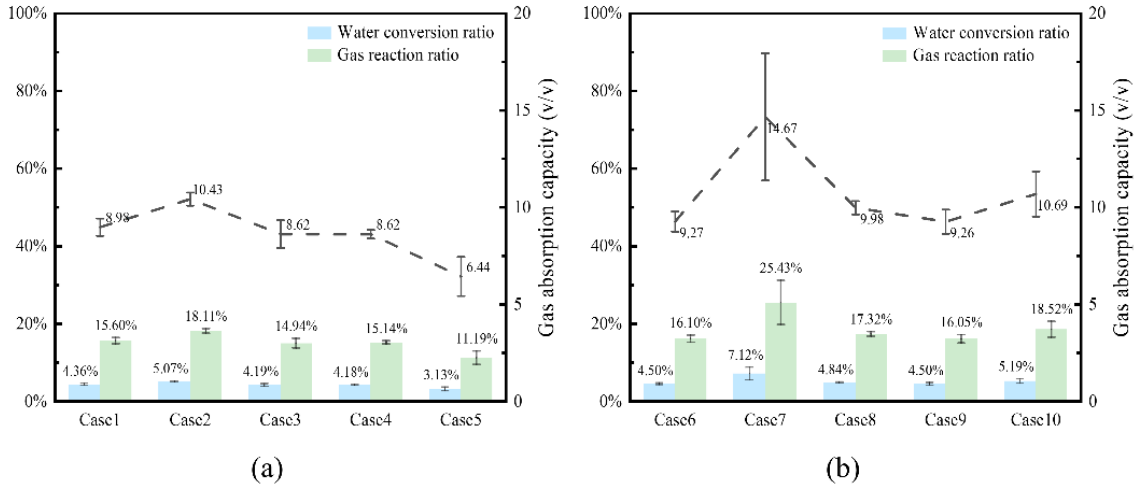

Figure 5. Effects of different masses of $Ca(OH)_2$ and SDS on water conversion ratio, gas reaction ratio, and gas absorption capacity: (a) varying $Ca(OH)_2$ mass; (b) varying SDS mass.

4.2. Effect of Composite Additives on CO_2 Hydrate Formation

In the composite system, the effects of different concentrations of $Ca(OH)_2$ and SDS on CO_2 hydrate formation were investigated. The detailed experimental conditions are listed in Table 3.

Table 3. Experimental conditions for composite systems.

Experiment	H_2O Mass (g)	SDS Mass (g)	$Ca(OH)_2$ Mass (g)	Temperature (°C)	Pressure (MPa)
Case 11	50	0.005	1	2	3.6
Case 12	50	0.01	1	2	3.6
Case 13	50	0.05	1	2	3.6
Case 14	50	0.1	1	2	3.6
Case 15	50	0.3	1	2	3.6
Case 16	50	0.05	0.05	2	3.6
Case 17	50	0.05	0.1	2	3.6
Case 18	50	0.05	0.5	2	3.6

The induction time of hydrate formation in the composite system is shown in Figure 6. In the $Ca(OH)_2$–SDS system, the addition of 0.05 g SDS at different $Ca(OH)_2$ loadings slightly increases the induction time compared to the system with $Ca(OH)_2$ alone, with an increase ranging from 14 to 57 minutes. This can be attributed to the adsorption of SDS on the surface of $CaCO_3$ particles, which reduces the carbonate characteristics of the particle surface and weakens its promoting effect on hydrate nucleation, thereby slightly prolonging the induction time. In addition, the presence of SDS leads to a reduction in $CaCO_3$ particle size, and smaller promoter particles are known to result in longer induction times [30].

However, under the condition of 0.05 g SDS and 1 g $Ca(OH)_2$, the induction time is significantly reduced. This may be due to the fact that SDS imparts surface activity to $CaCO_3$ particles originally located at the gas–liquid interface, enabling better dispersion. As a result, the dense $CaCO_3$ film formed at the interface is disrupted, reducing interfacial mass transfer resistance and effectively shortening the induction time.

For composite systems with different SDS concentrations, the induction time is significantly reduced compared to systems with SDS alone, mainly due to the introduction of $Ca(OH)_2$. After adding $Ca(OH)_2$, the $CaCO_3$ particles formed from its reaction with CO_2 can effectively promote hydrate nucleation, thereby greatly shortening the induction time,

which is consistent with the mechanism observed in the system with $Ca(OH)_2$ alone. However, the presence of SDS partially weakens the promoting effect of $CaCO_3$ particles on reducing the induction time.

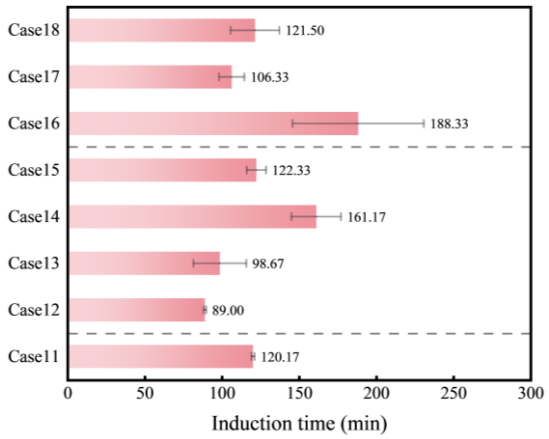

Figure 6. *Influence of $Ca(OH)_2$–SDS composite systems with varying masses on the induction time of CO_2 hydrate formation.*

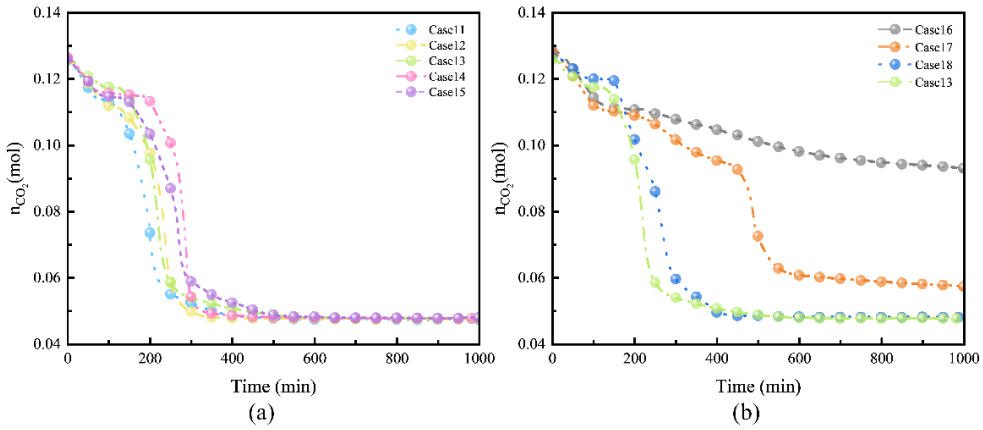

Figure 7. *Variation of CO_2 amount in the reactor under combined $Ca(OH)_2$–SDS systems with different mass ratios: (a) 1 g $Ca(OH)_2$ with varying SDS mass; (b) 0.05 g SDS with varying $Ca(OH)_2$ mass.*

Figure 7 presents the variation of CO_2 amount in the reactor over time for composite systems with different $Ca(OH)_2$ loadings at a fixed SDS concentration of 0.05 g. The results indicate that the amount of $Ca(OH)_2$ has a significant influence on CO_2 hydrate formation. Under the condition of 0.05 g SDS–0.05 g $Ca(OH)_2$, the decrease in CO_2 amount is limited and proceeds slowly. As the $Ca(OH)_2$ dosage increases, the CO_2 consumption increases; however, this relationship is non-linear. When the $Ca(OH)_2$ dosage exceeds 0.5 g, the final amount of CO_2 in the reactor no longer decreases significantly. At $Ca(OH)_2$ dosages of 0.5 g and 1 g, the final CO_2 amount reaches approximately 0.048 mol, which is significantly lower than that in single-additive systems and pure water. Meanwhile, the CO_2 consumption rate increases with increasing $Ca(OH)_2$ dosage. At 0.05 g $Ca(OH)_2$, CO_2 consumption occurs throughout almost the entire experimental period. When the dosage increases to 0.1 g, the CO_2 amount stabilizes after approximately 600 min, with a rapid hydrate formation stage occurring around 450 min. With further increases in $Ca(OH)_2$, CO_2 is rapidly consumed within 150–300 min and reaches a stable value at around 400 min until the end of the experiment. In addition, the figure also shows the variation of CO_2 amount with time for systems with different SDS concentrations combined with 1 g $Ca(OH)_2$. The results indicate that although the final CO_2 amount is nearly the same under different SDS concentrations, the time required to reach equilibrium varies. For instance, under the condition of 0.01 g SDS–1 g $Ca(OH)_2$, the CO_2 amount stabilizes at approximately 350 min.

Figure 8 presents the CO_2 consumption and consumption rate during the experiment. The gas consumption rate curve has been smoothed, therefore the maximum gas consumption rate cannot be reflected in the graph. Table 4 shows the maximum rate of carbon dioxide consumption and the final amount consumed. Under the condition of 0.05 g SDS–0.05 g $Ca(OH)_2$, the CO_2 consumption is approximately 0.01 mol higher than that of the system with 0.05 g $Ca(OH)_2$ alone. This enhancement is attributed to the addition of SDS, which promotes hydrate formation and increases CO_2 consumption.

However, the maximum CO_2 consumption rate under this condition is only 0.2 mmol·min^{-1}, mainly occurring during the cooling stage. This is likely due to the low $Ca(OH)_2$ dosage, resulting in a limited number of $CaCO_3$ particles available for SDS adsorption, thereby restricting hydrate growth. With increasing $Ca(OH)_2$ dosage, the hydrate formation behavior changes significantly. When 0.05 g SDS is combined with 0.1 g $Ca(OH)_2$, a peak gas consumption rate of 0.9 mmol·min^{-1} appears at approximately 500 min, which is much higher than that observed during the cooling stage, indicating rapid hydrate formation. This can be attributed to the presence of abundant hydrophobic particles, which facilitate the formation of cage-like water structures near the particle surface. In addition, the adsorption of CO_2 molecules on the particle surface provides sufficient guest molecules, thereby significantly enhancing the hydrate formation rate. Under this condition, hydrate formation is essentially completed at around 600 min, after which the system stabilizes, with minor hydrate formation occurring between 150 and 400 min, corresponding to relatively low gas consumption rates. When the $Ca(OH)_2$ dosage increases to 0.5 g, the total CO_2 consumption reaches 0.0784 mol, which is significantly higher than that in single-additive systems and pure water. The gas consumption rate exhibits two distinct peaks, at 0.44 mmol·min^{-1} and 0.79 mmol·min^{-1}, resulting in a longer time to reach equilibrium. The overall hydrate formation process takes approximately 250 min, slightly longer than the 150 min observed at 1 g $Ca(OH)_2$. With further increases in $Ca(OH)_2$ dosage, the total CO_2 consumption no longer increases and remains at approximately 0.0784 mol. However, the maximum gas consumption rate further increases to 1.4 mmol·min^{-1}, which is about 5.8 times higher than that of the system with $Ca(OH)_2$ alone. Meanwhile, the duration of the rapid hydrate formation stage is shortened to approximately 150 min. These results demonstrate that the $Ca(OH)_2$ dosage simultaneously influences both the total hydrate formation and the formation kinetics.

In the composite system, the total CO_2 consumption shows little variation under different SDS concentrations. Although some differences are observed in the CO_2 consumption rate, the maximum rate reaches 1.93 mmol·min^{-1}, which is approximately 6.4 times higher than that in the system with SDS alone. In addition, the duration required for the rapid hydrate formation stage is nearly the same across different conditions, at around 200 min. Overall, the influence of SDS concentration on CO_2 hydrate formation in the composite system is relatively limited. Even at low SDS concentrations, the surface of $CaCO_3$ particles can be effectively rendered hydrophobic, thereby promoting hydrate formation. Although this may slightly prolong the induction time, it does not significantly affect the final hydrate formation rate or the total CO_2 consumption.

Cheng et al. found that $CaCO_3$ and $Ca(HCO_3)_2$ formed from the reaction between $Ca(OH)_2$ and CO_2 in solution can provide additional nucleation sites, thereby promoting rapid hydrate nucleation and growth [27]. In addition, Cui et al. reported that $CaCO_3$ particles in aqueous solution are typically positively charged but do not exhibit significant surface activity. In the presence of SDS, SDS molecules adsorb onto the surface of $CaCO_3$ particles, neutralizing their surface charge and rendering the particles hydrophobic [33]. Farhang further demonstrated that hydrophobic particles can significantly enhance the kinetics of CO_2 hydrate formation. This is attributed to the reorganization of water molecules near hydrophobic surfaces into cage-like structures, as well as the enhanced adsorption and accumulation of gas molecules at the particle surface, which together facilitate hydrate nucleation [24]. Therefore, in the composite system investigated in this study, the significant enhancement in both CO_2 hydrate formation rate and yield can be attributed to the synergistic effects of increased nucleation sites and hydrophobic interfaces. On the one hand, $CaCO_3$ and $Ca(HCO_3)_2$ particles generated from the reaction between $Ca(OH)_2$ and CO_2 provide abundant nucleation sites, thereby accelerating hydrate nucleation. On the other hand, SDS induces hydrophobization of $CaCO_3$ particle surfaces, promoting the rearrangement of surrounding water molecules and facilitating the accumulation of gas molecules near the particle surface. Through the synergistic effects of these two mechanisms, the composite system significantly enhances both the formation rate and the total amount of CO_2 hydrate.

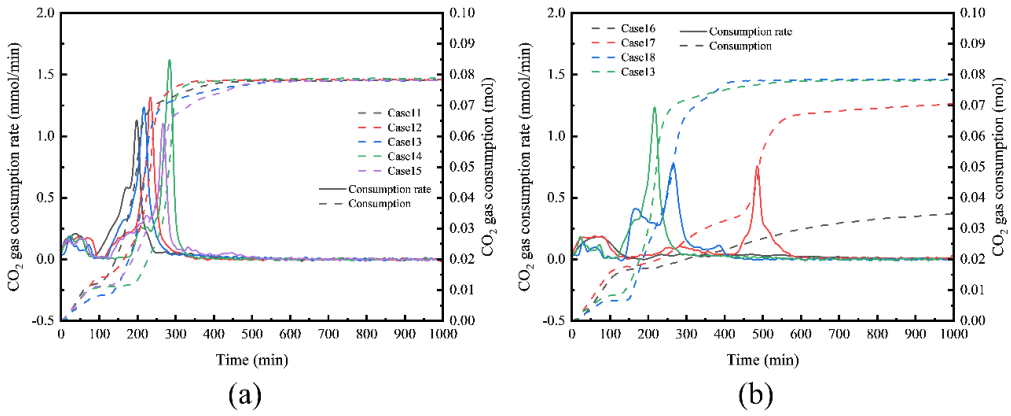

Figure 8. *Variation of CO_2 consumption and consumption rate under combined $Ca(OH)_2$–SDS systems with different mass combinations: (a) fixed $Ca(OH)_2$ (1 g) with varying SDS mass; (b) fixed SDS (0.05 g) with varying $Ca(OH)_2$ mass.*

Table 4. *Maximum rate of carbon dioxide consumption and final consumption.*

Experiment	Maximum carbon dioxide consumption (mmol·min^{-1})	carbon dioxide final consumption (mol)
Case11	1.32	0.078
Case12	1.71	0.078
Case13	1.4	0.078
Case14	1.93	0.079
Case15	1.26	0.078
Case16	0.19	0.035
Case17	0.9	0.071
Case18	0.79	0.078

Figure 9 presents the water conversion ratio, gas consumption ratio, and gas absorption capacity of CO_2 hydrates in the composite system. The results show that both the gas consumption ratio and water conversion ratio increase with increasing $Ca(OH)_2$ dosage. This is mainly attributed to the formation of more $CaCO_3$ and related species, which provide additional nucleation sites and thus promote hydrate formation.

However, further increasing the $Ca(OH)_2$ dosage does not lead to significant improvements in water conversion ratio or gas consumption ratio. This is mainly due to the formation of a hydrate layer at the gas–liquid interface, which hinders effective contact between CO_2 and water. In addition, the limited solubility of CO_2 in water restricts further gas consumption. Moreover, since the experiments were conducted under water-rich conditions, the continuous consumption of CO_2 leads to a decrease in system pressure, which also suppresses further hydrate formation.

Under the present experimental conditions, the maximum water conversion ratio and gas consumption ratio reach 17% and 62%, respectively, which are approximately 13% and 46% higher than those in the pure water system. The gas absorption capacity exhibits a similar trend, reaching a maximum value of 35.68 v/v, significantly outperforming the pure water system. Furthermore, when the $Ca(OH)_2$ dosage exceeds 0.5 g, the experimental results show good repeatability with small fluctuations, indicating excellent system stability and promising potential for practical applications.

In addition, the results indicate that SDS concentration has a relatively minor effect on water conversion ratio, gas consumption ratio, and gas absorption capacity in the composite system. Only a small amount of SDS is sufficient to achieve effective promotion, suggesting that SDS primarily plays a role in interfacial regulation rather than being a dominant controlling factor.

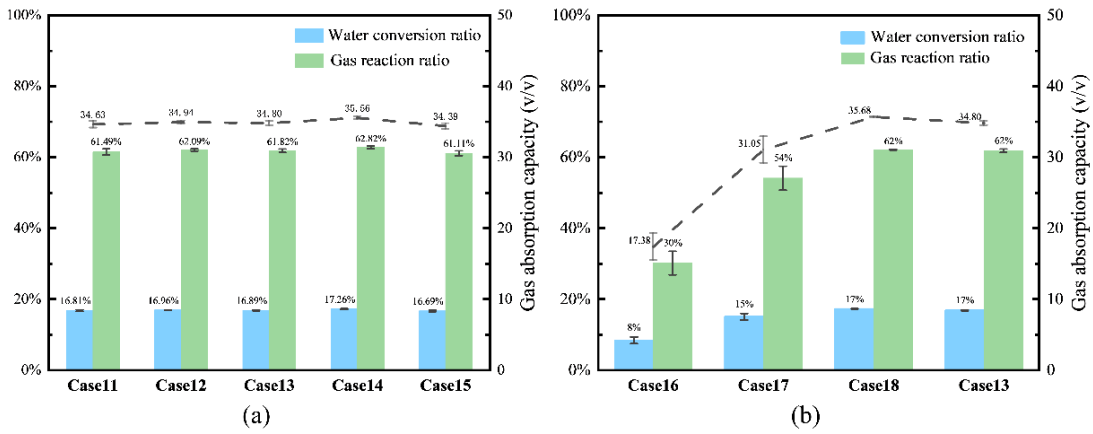

Figure 9. *Influence of $Ca(OH)_2$–SDS composite systems with varying mass combinations on water conversion ratio, gas reaction ratio, and gas absorption capacity: (a) fixed $Ca(OH)_2$ (1 g) with varying SDS mass; (b) fixed SDS (0.05 g) with varying $Ca(OH)_2$ mass.*

5. Conclusion

CO_2 hydrate is considered an efficient method for carbon sequestration. In this study, the synergistic promotion of CO_2 hydrate formation by $Ca(OH)_2$ and SDS was investigated based on the chemical reaction between $Ca(OH)_2$ and CO_2, which generates $CaCO_3$ as an intermediate promoting agent.

The results show that the addition of $Ca(OH)_2$ alone can shorten the induction time; however, it has a limited effect on enhancing hydrate formation rate and total gas consumption. Similarly, when SDS is used alone, the induction time depends on the SDS dosage, with the shortest induction time observed at 0.05 g SDS, but SDS alone does not significantly improve hydrate formation kinetics or capacity.

Compared with single-additive systems, the composite system of $Ca(OH)_2$ and SDS exhibits a markedly enhanced performance in CO_2 hydrate formation. Although the induction time is slightly prolonged, the hydrate formation rate and total CO_2 consumption are significantly improved. The results also indicate that variations in SDS dosage have a negligible effect on the overall promotion performance, whereas the dosage of $Ca(OH)_2$ plays a more critical role. At low $Ca(OH)_2$ loading (0.05 g), the hydrate formation amount is relatively limited. With increasing $Ca(OH)_2$ dosage, the hydrate formation is significantly enhanced; however, further increasing $Ca(OH)_2$ does not lead to additional improvement, indicating the existence of an optimal dosage range. Overall, the synergistic effect between $Ca(OH)_2$ and SDS enables simultaneous enhancement of nucleation and interfacial properties, thereby significantly improving both the kinetics and capacity of CO_2 hydrate formation.

Abbreviations

CCUS	Carbon Capture, Utilization and Storage
SDS	Sodium Dodecyl Sulfate
DTACI	Dodecyltrimethylammonium Chloride
LABS	Linear Alkylbenzene Sulfonate
CTAB	Cetyltrimethylammonium Bromide
ENP	Ethoxylated Nonylphenol
THF	Tetrahydrofuran
GO	Graphene Oxide

Acknowledgments

This study has been supported by the National Natural Science Foundation of China (Grant No. 52227812), the National Key R&D Program of China (Grant No. 2023YFB4104203), the Natural Science Foundation of Liaoning Province (Grant No. 2025JH6/101000002), and the Open Fund of State Key Laboratory of Coastal and Offshore Engineering with (Grant Nos. SL2502 and LY2503).

Author Contributions

Yaxiong Yang: Conceptualization, Writing – review & editing, Writing – original draft

Yuxin Jia: Data curation, Formal Analysis

Xiaolong Zhu: Methodology, Validation

Lei Yang: Conceptualization, Funding acquisition, Writing – review & editing

Yongchen Song: Supervision

Data Availability Statement

The data is available from the corresponding author upon reasonable request.

Conflicts of Interest

The authors declare no conflicts of interest.

References

[1] Yang SHB, Babu P, Chua SFS, et al. Carbon dioxide hydrate kinetics in porous media with and without salts. Applied Energy 2016; 162: 1131–40. https://doi.org/10.1016/j.apenergy.2014.11.052

[2] Lin W, Chen G-J, Sun C-Y, et al. Effect of surfactant on the formation and dissociation kinetic behavior of methane hydrate. Chemical Engineering Science 2004; 59: 4449–55. https://doi.org/10.1016/j.ces.2004.07.010

[3] Wang F, Jia Z-Z, Luo S-J, et al. Effects of different anionic surfactants on methane hydrate formation. Chemical Engineering Science 2015; 137: 896–903. https://doi.org/10.1016/j.ces.2015.07.021

[4] Du J, Li H, Wang L. Cooperative effect of surfactant addition and gas-inducing agitation on methane hydrate formation rate. Fuel 2018; 230: 134–7. https://doi.org/10.1016/j.fuel.2018.05.035

[5] Lo C, Zhang J, Somasundaran P, et al. Investigations of surfactant effects on gas hydrate formation via infrared spectroscopy. Journal of Colloid and Interface Science 2012; 376: 173–6. https://doi.org/10.1016/j.jcis.2012.03.012

[6] Du J, Li H, Wang L. Effects of ionic surfactants on methane hydrate formation kinetics in a static system. Advanced Powder Technology 2014; 25: 1227–33. https://doi.org/10.1016/j.apt.2014.06.002

[7] Kumar A, Sakpal T, Linga P, et al. Influence of contact medium and surfactants on carbon dioxide clathrate hydrate kinetics. Fuel 2013; 105: 664–71. https://doi.org/10.1016/j.fuel.2012.10.031

[8] Molokitina NS, Nesterov AN, Podenko LS, et al. Carbon dioxide hydrate formation with SDS: Further insights into mechanism of gas hydrate growth in the presence of surfactant. Fuel 2019; 235: 1400–11. https://doi.org/10.1016/j.fuel.2018.08.126

[9] Partoon B, Malik SNA, Azemi MH, et al. Experimental investigations on the potential of SDS as low-dosage promoter for carbon dioxide hydrate formation. Asia-Pacific J Chem Eng 2013; 8: 916–21. https://doi.org/10.1002/apj.1736

[10] Ganji H, Manteghian M, Sadaghiani Zadeh K, et al. Effect of different surfactants on methane hydrate formation rate, stability and storage capacity. Fuel 2007; 86: 434–41. https://doi.org/10.1016/j.fuel.2006.07.032

[11] Mohammadi M, Haghtalab A, Fakhroueian Z. Experimental study and thermodynamic modeling of CO_2 gas hydrate formation in presence of zinc oxide nanoparticles. The Journal of Chemical Thermodynamics 2016; 96: 24–33. https://doi.org/10.1016/j.jct.2015.12.015

[12] Jiao L, Wan R, Wang Z. Experimental investigation of CO2 hydrate formation in silica nanoparticle system under static conditions. Journal of Crystal Growth 2022; 583: 126539. https://doi.org/10.1016/j.jcrysgro.2022.126539

[13] Liu N, Li T, Liu T, et al. Molecular dynamics simulations of the effects of metal nanoparticles on methane hydrate formation. Journal of Molecular Liquids 2022; 356: 118962. https://doi.org/10.1016/j.molliq.2022.118962

[14] Aliabadi M, Rasoolzadeh A, Esmaeilzadeh F, et al. Experimental study of using CuO nanoparticles as a methane hydrate promoter. Journal of Natural Gas Science and Engineering 2015; 27: 1518–22. https://doi.org/10.1016/j.jngse.2015.10.017

[15] Wu Y, Shang L, Pan Z, et al. Gas hydrate formation in the presence of mixed surfactants and alumina nanoparticles. Journal of Natural Gas Science and Engineering 2021; 94: 104049. https://doi.org/10.1016/j.jngse.2021.104049

[16] Wang Y, Che X, Jiang X, et al. Investigation on CO_2 Hydrate Formation Promoted by Combination of Nanoparticles AlO(OH), ZnO, and TBAB. Energy Fuels 2024; 38: 22997–3008. https://doi.org/10.1021/acs.energyfuels.4c04292

[17] Mohammadi A, Manteghian M, Haghtalab A, et al. Kinetic study of carbon dioxide hydrate formation in presence of silver nanoparticles and SDS. Chemical Engineering Journal 2014; 237: 387–95. https://doi.org/10.1016/j.cej.2013.09.026

[18] Zhou S, Yu Y, Zhao M, et al. Effect of Graphite Nanoparticles on Promoting CO_2 Hydrate Formation. Energy Fuels 2014; 28: 4694–8. https://doi.org/10.1021/ef5000886

[19] Liu N, Chen L, Liu C, et al. Experimental study of carbon dioxide hydrate formation in the presence of graphene oxide. Energy 2020; 211: 118994. https://doi.org/10.1016/j.energy.2020.118994

[20] McElligott A, Uddin H, Meunier J-L, et al. Effects of Hydrophobic and Hydrophilic Graphene Nanoflakes on Methane Hydrate Kinetics. Energy Fuels 2019; 33: 11705–11. https://doi.org/10.1021/acs.energyfuels.9b02927

[21] Guo D, Ou W, Ning F, et al. Effects of hydrophilic and hydrophobic nano-CaCO3 on kinetics of hydrate formation. Energy Science & Engineering 2022; 10: 507–24. https://doi.org/10.1002/ese3.1042

[22] Nguyen NN, Nguyen AV, Steel KM, et al. Interfacial Gas Enrichment at Hydrophobic Surfaces and the Origin of Promotion of Gas Hydrate Formation by Hydrophobic Solid Particles. J Phys Chem C 2017; 121: 3830–40. https://doi.org/10.1021/acs.jpcc.6b07136

[23] Min J, Kang DW, Lee W, et al. Molecular Dynamics Simulations of Hydrophobic Nanoparticle Effects on Gas Hydrate Formation. J Phys Chem C 2020; 124: 4162–71. https://doi.org/10.1021/acs.jpcc.9b11459

[24] Farhang F, Nguyen AV, Sewell KB. Fundamental Investigation of the Effects of Hydrophobic Fumed Silica on the Formation of Carbon Dioxide Gas Hydrates. Energy Fuels 2014; 28: 7025–37. https://doi.org/10.1021/ef5009133

[25] Deng Z, Fan S, Wang Y, et al. High storage capacity and high formation rate of carbon dioxide hydrates via super-hydrophobic fluorinated graphenes. Energy 2023; 264: 126045. https://doi.org/10.1016/j.energy.2022.126045

[26] Gao P, Wu X, He Q, et al. The multidimensional optimization effects of L-serine in the mineralization of carbide slag with resultant controllable synthesis of novel and unique CaCO3 morphologies. Chemical Engineering Journal 2025; 513: 162935. https://doi.org/10.1016/j.cej.2025.162935

[27] Cheng C, Zhang J, Wang F, et al. Carbon dioxide hydrate formation synergistically enhanced by calcium hydroxide and tetrafluoroethane under low-pressure conditions. Chemical Engineering Journal 2025; 505: 159610. https://doi.org/10.1016/j.cej.2025.159610

[28] Shi C, Chai F, Yang M, et al. Enhance methane hydrate formation using fungus confining sodium dodecyl sulfate solutions for methane storage. Journal of Molecular Liquids 2021; 333: 116020. https://doi.org/10.1016/j.molliq.2021.116020

[29] Kumar R, Englezos P, Moudrakovski I, et al. Structure and composition of CO2 /H2 and CO2 /H2 /C3 H8 hydrate in relation to simultaneous CO2 capture and H2 production. AIChE Journal 2009; 55: 1584–94. https://doi.org/10.1002/aic.11844

[30] Nesterov AN, Reshetnikov AM, Manakov AYu, et al. Promotion and inhibition of gas hydrate formation by oxide powders. Journal of Molecular Liquids 2015; 204: 118–25. https://doi.org/10.1016/j.molliq.2015.01.037

[31] Han S-J, Yoo M, Kim D-W, et al. Carbon Dioxide Capture Using Calcium Hydroxide Aqueous Solution as the Absorbent. Energy Fuels 2011; 25: 3825–34. https://doi.org/10.1021/ef200415p

[32] Durán-Álvarez A, Maldonado-Domínguez M, González-Antonio O, et al. Experimental–Theoretical Approach to the Adsorption Mechanisms for Anionic, Cationic, and Zwitterionic Surfactants at the Calcite–Water Interface. Langmuir 2016; 32: 2608–16. https://doi.org/10.1021/acs.langmuir.5b04151

[33] Cui Z-G, Cui Y-Z, Cui C-F, et al. Aqueous Foams Stabilized by in Situ Surface Activation of CaCO3 Nanoparticles via Adsorption of Anionic Surfactant. Langmuir 2010; 26: 12567–74. https://doi.org/10.1021/la1016559